

Acrylic polymer influence on the structure and morphology of AgNPs obtained by chemical method for antimicrobial applications

Alexandra Pica, Cornelia Guran, Denisa Ficai,
Anton Ficai, Florica Dumitru

© American Coatings Association 2015

Abstract In this article, we present the synthesis of small silver nanoparticles (AgNPs) with an average size of 1–20(50) nm. Three formulations of AgNPs-based materials have been obtained and characterized by varying the weight ratio of the silver nitrate/acrylic polymer. AgNPs were prepared by simple chemical reduction method. The reduction of AgNO₃ was done by sodium borohydride in the presence of acrylic polymer, which acts also as a capping agent of AgNPs, avoiding the use of additional protective agents. The elemental analysis of AgNPs was quantified by X-ray fluorescence. The morphology and size of AgNPs were characterized by SEM and TEM–HRTEM, while the colloidal stability of AgNPs was demonstrated by zeta potential measurements. The influence of acrylic polymer on the stability of AgNPs, the particle sizes, and their antimicrobial efficacy was investigated. The results confirm that the introduction of acrylic polymer during the synthesis, acting as a stabilizing agent, increases the colloidal stability and antimicrobial performances of these formulations.

Keywords Nanoparticles, Antimicrobial performances, Colloidal stability

Introduction

Silver has been in use since time immemorial in the form of metallic silver, silver nitrate, and silver sulfadiazine for the treatment of burns, wounds, and several bacterial infections. But due to the emergence of several antibiotics the use of these silver compounds has declined remarkably. Nanotechnology is gaining tremendous impetus in the present century due to its capability of modulating metals into nanosize, which drastically changes the chemical, physical, and optical properties of metals. Metallic silver in the form of silver nanoparticles (AgNPs) has made a remarkable comeback as a potential antimicrobial agent. The use of AgNPs is also important, as several pathogenic bacteria have developed resistance to various antibiotics.^{1,2} The antimicrobial activity of AgNPs may be related to several mechanisms including induction of oxidative stress due to generation of reactive oxygen species (ROS), which may cause the degradation of the membrane structure of the cell and release of ions from the surface of nanoparticles that has been reported to cause bacterial death due to binding to cell membrane. However, the mechanism of toxicity is still only partially understood.^{3,4} AgNPs can damage cell membranes of microorganisms by forming “pits” on their surfaces. Moreover, they may penetrate into the cells to cause DNA damage. Silver ions released from the surface of these nanoparticles can interact with thiol groups in protein to induce bacterial inactivation, condensation of DNA molecules, and loss of their replication ability.⁵ Recently, inorganic nanoparticles protected by organic ligands have attracted much interest due to their diverse technological applications.⁶

Metal nanoparticles represent a new class of materials that are increasingly being developed for their use in research and health-related applications. Metallic ions are interesting not only for their wide variety of

A. Pica (✉), C. Guran, D. Ficai, A. Ficai
Politehnica University of Bucharest, 1-7 Polizu St.,
011061 Bucharest, Romania
e-mail: alexpica02@yahoo.com

F. Dumitru
Research Institute for Advanced Coatings, 49A Theodor
Pallady Bvd., Bucharest, Romania
e-mail: florica.dumitru@icaaro.com

physical and chemical properties but also for their antibacterial activity.⁷

AgNPs have been evaluated for their antimicrobial activities against a wide range of pathogenic organisms.^{8–13} The highest sensitivity was observed against Methicillin-resistant *Staphylococcus aureus* (MRSA) followed by Methicillin-resistant *Staphylococcus epidermidis* (MRSE) and *Streptococcus pyogenes*. A moderate antimicrobial activity was observed in the cases of the gram-negative pathogens *Salmonella typhi* and *Klebsiella pneumoniae*.¹⁴

Small particles exhibited higher antimicrobial activity than large particles. This result can be due to high particle penetration when these particles have smaller sizes. The antibacterial properties are related to the total surface area of the nanoparticles. Smaller particles with larger surface-to-volume ratios have greater antibacterial activity.^{15–18}

In this work, AgNPs were synthesized by simple chemical reduction method in the presence of acrylic polymer. The effects of concentrations of acrylic polymer were studied in detail. The AgNPs were characterized by X-ray fluorescence (XRF) spectroscopy, UV–Vis, and SEM.

The antibacterial effects of AgNPs on the gram-positive and gram-negative bacteria were investigated. Our results signify that the AgNPs synthesized by chemical reduction method are suitable for formulation of new types of antimicrobial materials.

Experimental methods and materials

Materials

All the chemicals were of analytical grade: AgNO₃ and NaBH₄ supplied by Sigma-Aldrich, acrylic polymer Plextol D 498 from Synthomer, and propylene glycol supplied by OLTCHIM.

Equipment

XRF is a common analytical technique which can be used for qualitative and quantitative determination of the elements between calcium and uranium. The elemental composition of AgNPs1–AgNPs3 was determined with an X-MET handheld device TXR 3000 using an X-ray source of rhodium. The analysis method was *alloy-fp*. The instrument measures the elemental composition of elements on the surface of the sample and very little depending on the power of penetration depth of X-rays in the material which depends on Z-average material.

UV–Vis spectra were recorded on a Hitachi High Technologies America, San Jose, CA spectrometer. The model U-0080D photodiode-array spectrophotometer, designed to meet the requirements of biotechnology laboratories, is equipped with standard DNA/

RNA analysis software. The spectrophotometer reportedly is capable of measuring the entire wavelength range within 0.05 s.

SEM analysis for AgNPs was performed on a Nova NanoSEM 630 (Field Emission Gun Scanning Electron Microscope—ultra-high-resolution characterization; beam deceleration mode with sub-100 V and high surface sensitivity imaging; 150 × 150 mm² high-precision and stability piezostage).

Nanosizer 90 Plus Brookhaven was used for the measurement of zeta potential. Scattered light intensity fluctuations are analyzed by particles in Brownian motion to obtain an average size of polydispersion and to obtain a full distribution.

(High-resolution) transmission electron microscopy—(HR)TEM—investigations were performed using a Titan ChemiSTEM 80–200 kV probe Cs corrected microscope equipped with a Super-X EDS System. Low-magnification TEM and high-resolution TEM (HRTEM) images were acquired with a Gatan UltraScan 1000 P camera controlled with a Digital Micrograph software integrated in the microscope's user interface. STEM images were acquired with a high-angle annular dark field (HAADF) detector. The alignment of the microscope was carried out through the Cs DCOR probe corrector software.

Synthesis of silver nanoparticles

Kinetics of processes taking place in the chemical synthesis of AgNPs are not well known because they are very complex and overlapping processes. Therefore, both nanoparticle shapes and sizes cannot be controlled simultaneously. Nanoparticles with high specific surfaces tend to agglomerate and form clusters or to grow, forming larger particles.¹⁹ Agglomeration of fine particles can occur during synthesis, drying, and further processing of the particles, so in every step it is necessary to take care about the stabilization of the particles against agglomeration. Nanoparticle agglomeration is caused by van der Waals forces and/or driving forces that tend to minimize the total surface energy of the system.²⁰ To avoid the agglomeration of the nanoparticles, the synthesis has to take place, preferably in the presence of a polymer.

Synthetic polymers stabilized nanoparticle surface avoiding agglomeration by the presence in their structure of long-chain hydrocarbon moieties. AgNPs used in our experiments were synthesized by chemical reduction method in the presence of an acrylic polymer.

The choice of the polymer was based on the following:

- Antibacterial effectiveness of the composite polymer/AgNPs against *Escherichia coli* and *S. aureus*.
- Effectiveness of the dispersion of AgNPs.
- The mobility of silver ions in the polymer material in the presence of acrylic acid.

The synthesis of AgNPs was performed in two stages:

- Stage I: synthesis of AgNPs by heterogeneous nucleation and
- Stage II: seed and feed grown particles.

The synthesis of AgNPs was done as follows. First of all, 250 mL of 0.005 M AgNO₃ was mixed with 125 mL solution-acrylic polymer (Plextol D 498 –50% water/propylene glycol). The mixture was stirred for 10 min at 20–23°C and then quickly added to 44 mL aqueous solution of 2.0×10^{-3} M NaBH₄, maintaining the

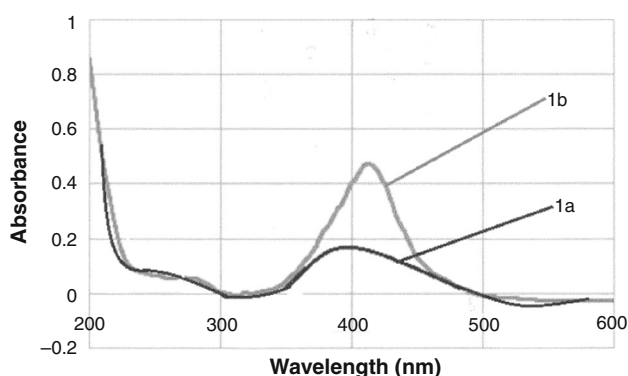


Fig. 1: (a) UV-Vis spectrum of silver nanoparticles (stage 1) and (b) UV-Vis spectrum of silver nanoparticles after seed and feed (stage II)

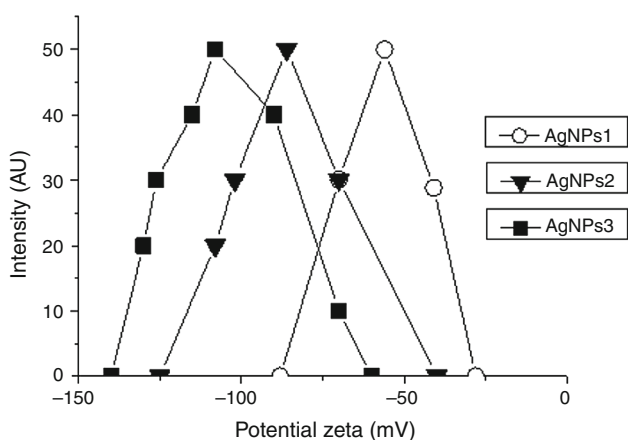


Fig. 2: Zeta potential for AgNPs1–AgNPs3

resulting mixture stirred vigorously for 20 min. During mixing of the solutions, Ag ions are reduced and agglomerated, forming monodispersed nanoparticles in aqueous medium. According to Fig. 1a, the solutions exhibited a surface plasmon resonance absorption band with average maximum wavelength at around 400 nm, indicating the formation of a small number of AgNPs. The particles were purified by precipitation in hexane and then dried. Dried nanoparticles were then washed with 80 mL of distilled water to remove the excess of unreacted NaBH₄.

Seed and feed

Germes were also prepared by dissolving 44.8 mg propylene glycol in 20 mL acrylic polymer; then 12.2 mg AgNO₃ dissolved in 0.05 ml of water was added, and the solution was allowed to stir for 1 h. The last step was represented by the addition of 30.8 mg of NaBH₄ dissolved in 1 ml of distilled water. A dark brown solution resulted, which highlights the formation of AgNPs. The solution was centrifuged at 10,000 rpm for 20 min. The particles were rinsed with water, filtered, and dried. As shown in Fig. 1b, the intensity of the peak at 416 nm increased, indicating the formation of a larger number of AgNPs.

The important advantage is that the AgNPs prepared by this simple reduction process remain stable for 1 month without any agglomeration. By this method, three samples denoted by AgNPs1–AgNPs3 were prepared and are presented in Table 1.

Antimicrobial activity using a time-kill procedure

The antimicrobial activity of AgNPs was tested by following the Time-Kill Procedure, adapting and integrating the protocols described in the standard ASTM E2315 (Assessment of Antimicrobial Activity Using a Time-Kill Procedure). The activity of the test material is quenched at specified sampling intervals (for example, 15 and 30 min, 1 and 2 h).

AgNPs were diluted at 3 different concentrations in sterile distilled water (1.221, 0.308, and 0.083 µg/mL, respectively). Each AgNPs suspension was inoculated with an *E. coli* (106 cfu/mL).

At the same time, different concentrations of AgNPs in sterile distilled water (19.53, 4.788, and

Table 1: Synthesis conditions of AgNPs samples

Sample	AgNO ₃ /acrylic polymer (w/w)	NaBH ₄ concentration [M]	AgNO ₃ concentration [M]
AgNPs1	5:1.5	2×10^{-3}	0.005
AgNPs2	5:2	2×10^{-3}	0.005
AgNPs3	5:2.5	2×10^{-3}	0.005

Table 2: Zeta potential domains and corresponding colloidal stability vs zeta potential of synthesized AgNPs_x (x = 1–3)

Zeta potential domain (mV)	Stability behavior of the colloid	Experimental zeta potential of AgNPs _x (x = 1–3) (mV)
[–5 to +5]	Rapid coagulation or flocculation	–
(–10,–5) and (+5,+10)	Incipient instability	–
(–40,–10) and (+10,+40)	Moderate stability	–
([–60,–40) and (+40,+60)	Good stability	–56 (AgNPs ₁); –86 (AgNPs ₂)
<–60 or >60	Excellent stability	–108 (AgNPs ₃)

0.308 µg/mL, respectively) were also used to inoculate with the *S. aureus* (106 CFU/mL).

The samples were incubated at the temperature 25 ± 2°C for 24–48 h for each organism selected. Incubation time should allow for the growth of surviving organisms, without overgrowth of colonies.

Results and discussions

The colloidal stability of silver nanoparticles in aqueous solution

The stability of colloidal dispersions is closely related to size and zeta potential. Zeta potential can be correlated with the degree of repulsion between adjacent particles, similarly charged in a dispersion. For colloidal molecules and particles, a high zeta potential will confer stability, and the solution or dispersion will avoid aggregation. When the potential is low, attraction between particles is greater, which may lead to flocculation or aggregation. Therefore, colloids with high zeta potential (negative or positive) are electrically stabilized, while colloids with low zeta potential tend to coagulate (see Table 2).²¹

Since the ultimate goal of this research is to obtain antimicrobial film-forming materials, we should choose a method for obtaining AgNPs, leading to their homogeneous distribution in the polymer matrix. For these reasons, we choose as solution the chemical synthesis of AgNPs in acrylic polymer Plextol D 498. The research so far revealed that when the acrylic acid has been used to stabilize AgNPs, the composites obtained showed antibacterial efficacy against *E. coli* and *S. aureus*. It appears that the acrylic acid induces the mobility of silver ions in the film-forming material, which leads to a good dispersion of nanoparticles into an organic matrix.^{22,23} The dispersion of AgNPs was carried out in distilled water in the presence of propylene glycol and acrylic polymer as follows: in a glass flask 100 mL of distilled water, 2.8 g propylene glycol, and 1.2 g of acrylic polymer were added and stirred magnetically for 5 min at pH 9 (the pH correction was done with ammonia, 25%). Then, 10 g of AgNPs powder was added under magnetic stirring at a rate of 1 g AgNPs/10 min followed by further stirring for 2 h. The zeta potential of the three AgNPs samples is presented in Fig. 2.

Table 3: Correlation of AgNPs_x size (x = 1–3) with the AgNO₃: acrylic polymer

Sample	AgNO ₃ /acrylic polymer (w:w)	Average size (nm)
AgNPs ₁	5:1.5	50
AgNPs ₂	5:2	16
AgNPs ₃	5:2.5	14

The stabilizing effect of organic compounds was also studied according to the literature data. The AgNPs obtained in water were unstable (the size is ~65 nm while the zeta potential is close to 0).²⁴

In the presence of acrylic polymer, the surface charge decreases to –108 mV and consequently the agglomeration is strongly reduced (see Fig. 2 and Table 2).

The presence of acrylic polymer used as a capping agent for AgNPs leads to a higher zeta potential. Based on the zeta potential data, it can be supposed that AgNPs are surrounded by acrylic polymer, thus avoiding the agglomerates. Note that AgNPs₃ shows the highest value of the zeta potential which gives excellent colloidal stability. All three samples have a negative surface charge with a zeta potential in the range of –56 to –108 mV.

Morphological assessments

SEM

Morphological assessments of AgNPs_{1–3} were performed by scanning electron microscopy technique (SEM). The influence of polymer on the size of AgNPs is presented in Table 3.

The size and distribution of the AgNPs depend on the weight ratio of AgNO₃/acrylic polymer. It can be observed that most AgNPs have an average size of particles between 14 and 16 nm. In Fig. 3, the micrographs of AgNPs obtained after 48 h from the beginning of the synthesis, for different weight ratios of AgNO₃/acrylic polymer, are shown. For a weight ratio of 5:2.5, it can be said that small nanoparticles were formed as spheres uniformly distributed. As the weight ratio of AgNO₃/acrylic polymer increases, larger

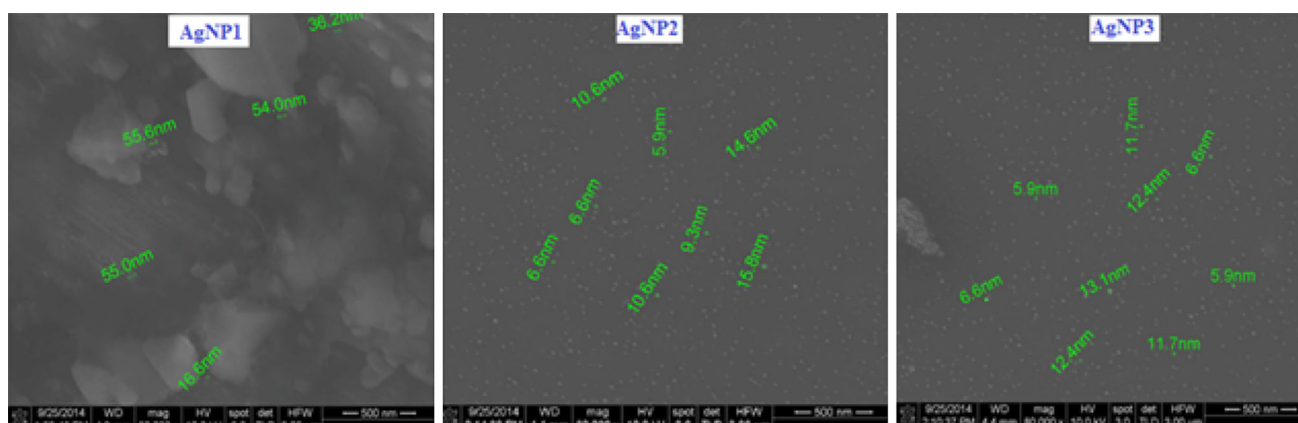


Fig. 3: SEM micrographs of AgNPs

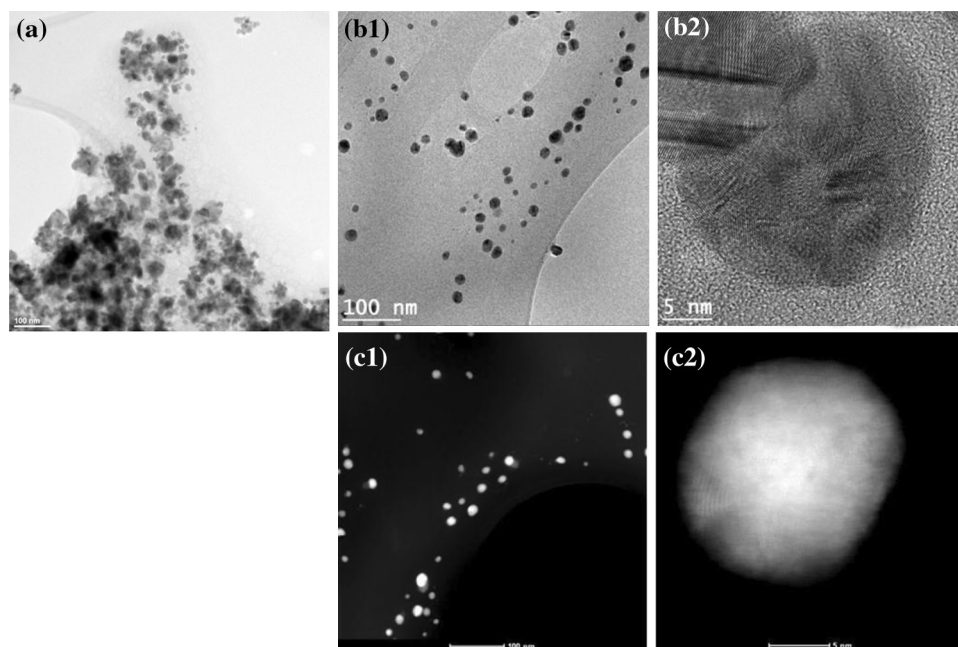


Fig. 4: TEM image of AgNPs0 (a), TEM–HRTEM images of AgNPs3 (b1,2), and HAADF STEM images of AgNPs3 (c1,2)

nanoparticles with an irregular surface are observed, while the proportion of small nanoparticles decreases. From SEM images, it is observed that for AgNPs1 large particles are obtained.

TEM and HRTEM

The analysis of the size and shape of AgNPs needs a more powerful tool compared with SEM. The transmission electron microscopy technique was used to visualize the size and shape of the synthesized AgNPs. Samples for TEM studies were prepared by dropping an ultrasonically dispersed solution of AgNPs onto a carbon-coated Cu grid. Figures 4 and 5 show that AgNPs are spherical in shape, having a smooth surface, and are well dispersed.

It is very important that AgNPs obtained in the presence of the acrylic polymer present very narrow size distribution (Figs. 4b1 and 4b2) with irregular shape and average size of ca. 15 nm (HRTEM image—Fig. 4b2 and HAADF STEM image—Fig. 4c2). For a better visualization, pure AgNPs (obtained in the absence of acrylic polymer, but under the same reduction conditions) are also presented and denoted with AgNPs0 (Fig. 4a). Figures 4c1 and 4c2 exhibit the high-angle annular dark field (HAADF) STEM image of the AgNPs3. As presented in Fig. 4c2, the surface is unclear, most probably due to the presence of polymer coating.

In a similar manner, TEM images of AgNPs2 exhibit spherical AgNPs. The TEM–HRTEM micrograph suggests that the average size of the AgNPs2 is a little bit larger than that of AgNPs3 and measures ~20 nm. For a weight ratio of 5:2.5 or 5:2, it can be said that

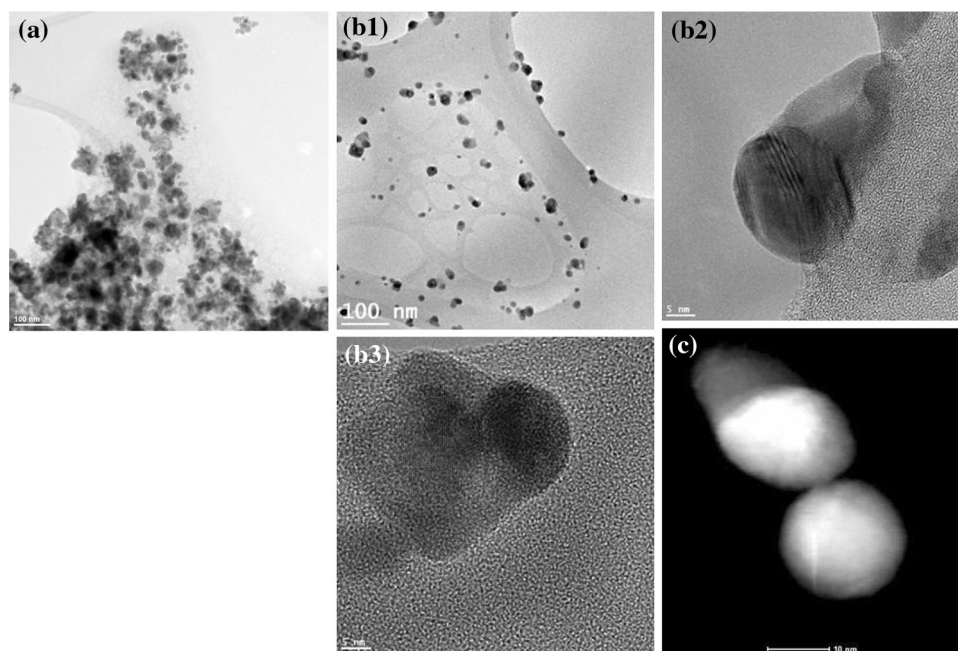


Fig. 5: TEM image of AgNPs0 (a), TEM-HRTEM images of AgNPs2 (b1–b3), and HAADF STEM images of AgNPs2 (c)

Table 4: Elemental composition of AgNPs (w:w)

Sample (%)	Ag (%)	Fe (%)	Cr (%)
AgNPs1	99.1	0.5	0.1
AgNPs2	99.1	0.4	0.1
AgNPs3	99.2	0.3	Traces

Elemental analysis of AgNPs using X-ray fluorescence

Each sample of AgNPs was measured for 60 s. The results are shown in Table 4 and Fig. 6, the purity of these samples being higher than 99%. The most abundant impurity is iron (0.3–0.5%), while chromium is below 0.1%.

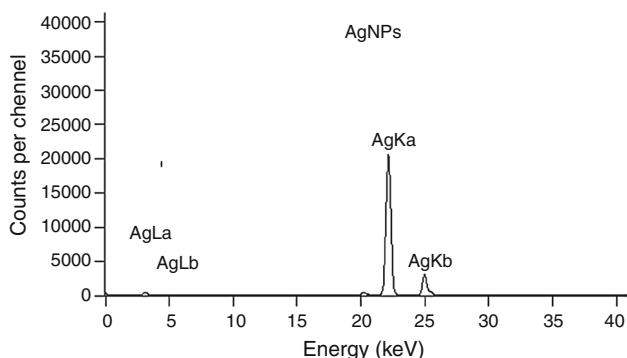


Fig. 6: XRF spectra of AgNPs

small nanoparticles with wider size distribution were formed. The pure AgNPs (AgNPsO) are shown in Fig. 4a or Fig. 5a. In STEM mode, the surface morphology of the AgNPs2 proves the presence of polymer coating on the surface of AgNPs.

Based on the literature data, the smaller particles showed higher antimicrobial activity.¹⁷

Antibacterial activity

The antibacterial activity of AgNPs was tested by following the Time-Kill Procedure. For this purpose, the samples were diluted to different concentrations in sterile distilled water. Each AgNP was inoculated with a bacterial suspension to a final cellular concentration of 10⁶ CFU/ml. After 15 and 30 min, and 1 and 2 h, an aliquot of each sample was removed, appropriately diluted in H₂O, and plated on a petri dish containing plate count agar.

The challenge bacteria tested were *S. aureus* (gram-positive) and *E. coli* (gram-negative), both cultured in Nutrient Broth Agar.

The results of the Time-Kill Test (expressed as microbial population Percent Reduction) are reported in Figs. 7 and 8, respectively, for *E. coli* and *S. aureus*.

All the AgNPs showed significant antibacterial activity against both analyzed microorganisms. AgNPs1–AgNPs3 showed a very similar antibacterial profile and overall a high antibacterial activity, demonstrating maximum microbial population reduction ($\geq 99.8\%$) at 1.221 $\mu\text{g/mL}$ and ($\geq 99.7\%$) at 0.308 $\mu\text{g/mL}$ on *E. coli* (Fig. 7). For low concentrations

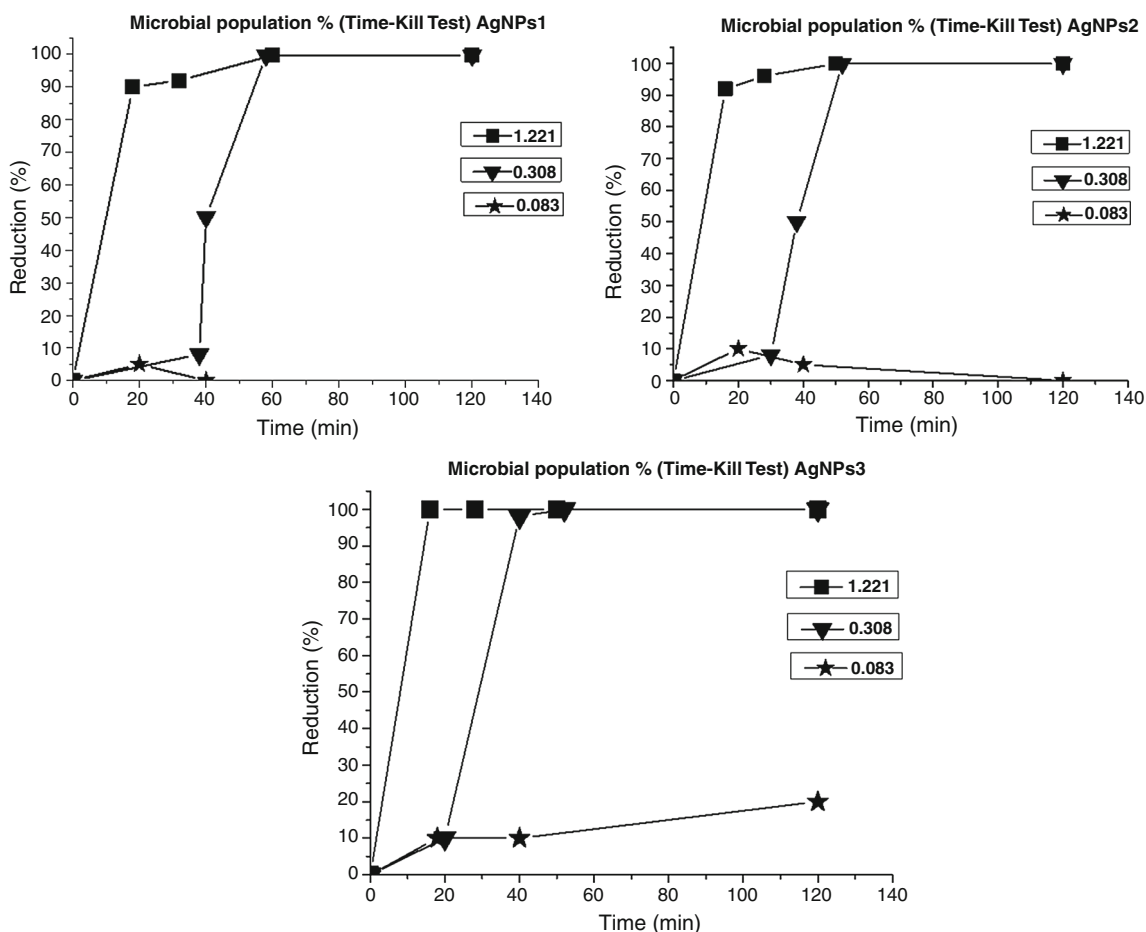


Fig. 7: Microbial population Percent Reduction of AgNPs1–AgNPs3 on *Escherichia coli* (gram-negative) evaluated by following the Time-Kill Test

(0.083 µg/mL), the bacterial population reduction is very small ($\geq 18\%$). In the case of *S. aureus*, a significant reduction in bacterial population ($\leq 99.93\%$) is observed for high concentrations of AgNPs (i.e., 19.52 and 4.388 mg/ml). It can be seen that at a concentration of AgNPs of 19.52 mg/ml, reduction of the bacterial population occurs much faster, i.e., after 20 min the killing of bacteria is of 90–95% (Fig. 8). To achieve a significant reduction (99.7%) of gram-negative bacteria (*E. coli*), the minimum concentration of AgNPs is 0.308 µg/mL. In the case of *S. aureus*, the minimum concentration of AgNPs is 4.388 mg/mL.

The antibacterial activity of Ag nanoparticles is closely related to the exposed surface to oxidation and particle dispersion. In order to achieve an antimicrobial film-forming material, it is important to effectively disperse Ag nanoparticles in the polymer matrix.

In general, the aqueous dispersions of polymers are susceptible to degradation due to microorganisms which are present in the water. Thus, Plextol D498 contains a biocide that provides antimicrobial protection of the polymer but only in the package (in-can

biocide). Usually, the content of in-can biocide is of 0.05–0.2% and is used mainly for bacterial growth inhibition during storage.²⁴ When the polymer is used in an organic coating for effective antibacterial activity, a supplement of biocide (in-film biocide) is required. However, the amount of polymer present on the surface of AgNPs is too small (not detected by XRF analysis, the detection limit of the device is 0.1%) and it is less likely that this biocide present in the polymer could influence the antimicrobial activity of AgNPs. Using the polymer Plextol D498 in the synthesis of AgNPs seems to influence instead the particle size and their yield of dispersion. These factors influence, in turn, the antimicrobial activity of AgNPs. As expected, the best antibacterial results were obtained with the AgNPs3 sample (size ~ 20 nm by TEM and ratio AgNO₃/acrylic polymer 5:2.5).

Conclusions

Uniform size of the AgNPs was successfully achieved from the AgNO₃ at different acrylic polymer concen-

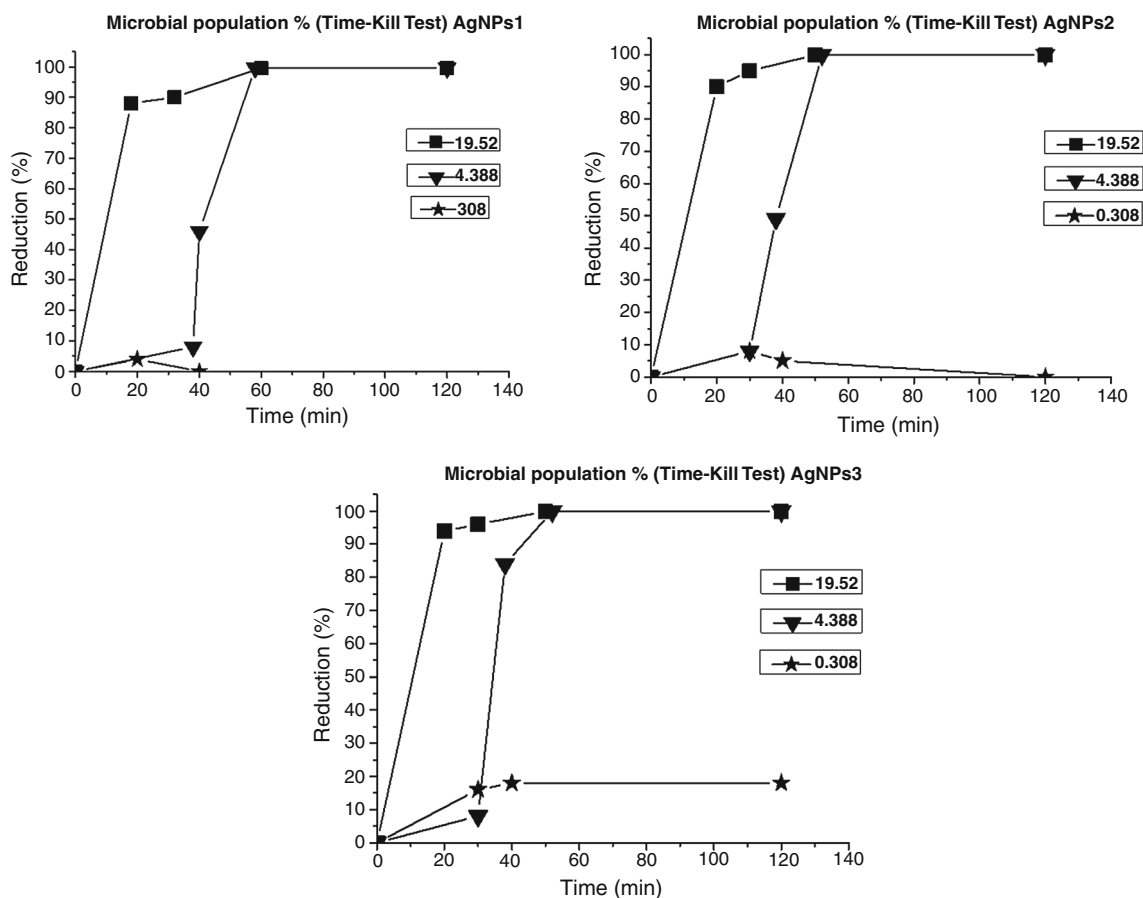


Fig. 8: Microbial population Percent Reduction of AgNPs1–AgNPs3 on *Staphylococcus aureus* (gram-positive) evaluated by following the Time-Kill Test

trations using sodium borohydride as a chemical reduction agent. The SEM, TEM, and HRTEM images show that the morphology of AgNPs1–AgNPs3 demonstrates spherical shapes with no noteworthy morphological distinctions between them. The only differences that occur are the size and yield of dispersion of the AgNPs. The reduction of the silver in the presence of the acrylic polymer is beneficial because the polymer acts as a growth inhibitor and also as an efficient dispersing agent. The synthesized AgNPs show antibacterial activity against gram-positive and gram-negative bacteria. The use of acrylic polymer in the synthesis of AgNPs as a stabilizing agent is beneficial for controlling the size and stability of the nanoparticles. On the other hand, the size and stability of NPs influence their antibacterial activity.

As the polymer content is higher, the potential is higher. These results show that the antibacterial activity of AgNPs can be changed with the size of AgNPs and concentration of acrylic polymer. The best results were obtained for AgNPs3, where the reduction of bacterial population was ~99.97%. Further studies will investigate the bactericidal effects of AgNPs on the types of bacteria and fungus for potential widening of this subject area, such as coatings and film-forming

materials, our final goal being to obtain antimicrobial coatings.

Acknowledgments The work has been funded by the Sectoral Operational Programme Human Resources Development 2007–2013 of the Ministry of European Funds through the Financial Agreement POSDRU/159/1.5/S/132395.

References

1. Xiu, Z, Zhang, Q, Puppala, HL, Colvin, VL, Alvarez, PJJ, “Negligible Particle-Specific Antibacterial Activity of Silver Nanoparticles.” *Nano Lett.*, **12** 4271–4275 (2012)
2. Abbass, H, *Advances in Nanocomposite Technology*. InTech, Rijeka, 2011
3. Emamifar, A, Kadivar, M, Shahedi, M, Solaimanianzad, S, “Effect of Nanocomposite Packaging Containing Ag and ZnO on Inactivation of *Lactobacillus plantarum* in Orange Juice.” *Food Control*, **22** (3–4) 408–413 (2011)
4. Dobias, J, Bernier-Latmani, R, “Silver Release from Silver Nanoparticles in Natural Waters.” *Environ. Sci. Technol.*, **47** 4140–4146 (2013)

5. Morones, JR, Elechiguerra, JL, Camacho, A, Holt, K, Kouri, JB, Ramírez, J, Sharaf, MA, “Formulation and Evaluation of Silver Nanoparticles as Antibacterial and Antifungal Agents with a Minimal Cytotoxic Effect.” *Int. J. Drug Deliv.*, **3** 293–304 (2011)
6. Das, R, Gang, S, Nath, SS, “Preparation and Antibacterial Activity of Silver Nanoparticles.” *J. Biomater. Nanobiotechnol.*, **2** 472–475 (2011)
7. Meyer, DE, Curran, MA, Gonzalez, MA, “An Examination of Silver Nanoparticles in Socks Using Screening-Level Life Cycle Assessment.” *J. Nanopart. Res.*, **13** 147–156 (2011)
8. Yamanaka, M, Hara, K, Kudo, J, “Bactericidal Actions of a Silver Ion Solution on *Escherichia coli*, Studied by Energy-Filtering Transmission Electron Microscopy and Proteomic Analysis.” *Appl. Environ. Microbiol.*, **71** 7589–7593 (2005)
9. Lara, HH, Nilda, VA, Turrent, LCI, Padilla, CR, “Bactericidal Effect of Silver Nanoparticles Against Multidrug-Resistant Bacteria.” *World J. Microbiol. Biotechnol.*, **26** 615–621 (2010)
10. Shahverdi, AR, Fakhimi, A, Shahverdi, HR, Minaian, S, “Synthesis and Effect of Silver Nanoparticles on the Antibacterial Activity of Different Antibiotics Against *Staphylococcus aureus* and *Escherichia coli*.” *Nanomed: Nanotechnol. Biol. Med.*, **3** 168–171 (2007)
11. Shrivastava, S, Bera, T, Roy, A, Singh, G, Ramachandrarao, P, Dash, D, “Characterization of Enhanced Antibacterial Effects of Novel Silver Nanoparticles.” *Nanotechnology*, **18** 1–9 (2007)
12. Yoon, K, Byeon, JH, Park, J, Hwang, J, “Susceptibility Constants of *Escherichia coli* and *Bacillus subtilis* to Silver and Copper Nanoparticles.” *Sci. Total Environ.*, **373** 572–575 (2007)
13. Sarkar, S, Jana, AD, Samanta, SK, Mostafa, G, “Facile Synthesis of Silver Nanoparticles with Highly Efficient Antimicrobial Property.” *Polyhedron*, **26** 4419–4426 (2007)
14. Nanda, A, Saravanan, M, “Biosynthesis of Silver Nanoparticles from *Staphylococcus aureus* and Its Antimicrobial Activity Against MRSA and MRSE.” *Nanomedicine*, **5** 452–456 (2009)
15. Cho, KH, Park, JE, Osaka, T, Park, SG, “The Study of Antimicrobial Activity and Preservative Effects of Nanosilver Ingredient.” *Electrochim. Acta*, **51** (5) 956–960 (2005)
16. Baker, C, Pradhan, A, Pakstis, L, Pochan, DJ, Shah, SI, “Synthesis and Antibacterial Properties of Silver Nanoparticles.” *J. Nanosci. Nanotechnol.*, **5** 244–249 (2005)
17. Nedelcu, IA, Ficai, A, Sonmez, M, Ficai, D, Oprea, O, Andronescu, E, “Silver Based Materials for Biomedical Applications.” *Curr. Org. Chem.*, **18** (2) 173–184 (2014)
18. Martínez-Castañón, GA, Niño-Martínez, N, Martínez-Gutiérrez, F, Martínez-Mendoza, JR, Ruiz, F, “Synthesis and Antibacterial Activity of Silver Nanoparticles with Different Sizes.” *J. Nanopart. Res.*, **10** 1343–1348 (2008)
19. Salem, AZM, El-Adawy, M, Gado, H, Camacho, LM, Ronquillo, M, Alsersy, H, Borhami, B, “Effects of Exogenous Enzymes on Nutrients Digestibility and Growth Performance in Sheep and Goats.” *Trop. Subtrop. Agroecosyst*, **14** 867–874 (2011)
20. Hunter, RJ, *Foundations of Colloid Science*. Oxford University Press, New York, 1989
21. http://en.wikipedia.org/wiki/Zeta_potential
22. Horkey, SM, Pearce, C, Murray, K, “Anti-Microbial Paint Films.” US Patent 20080233204, 2008
23. Quaroni, L, Chumanov, G, “Preparation of Polymer-Coated Functionalized Silver Nanoparticles.” *J. Am. Chem. Soc.*, **121** 10642–10643 (1999)
24. Khan, SS, Mukherjee, A, Chandrasekaran, N, “Impact of Exopolysaccharides on the Stability of Silver Nanoparticles in Water.” *Water Res.*, **45** (5) 184–5190 (2011)